Vol. 34 – N° 2 06 10 p. 117–134

GEOSTANDARDS and GEOANALYTICAL RESEARCH

Penglai Zircon Megacrysts: A Potential New Working Reference Material for Microbeam Determination of Hf–O Isotopes and U–Pb Age

Xian-Hua **Li** (1,2)*, Weng-Guo **Long** (2), Qiu-Li **Li** (1), Yu **Liu** (1), Yong-Fei **Zheng** (3), Yue-Heng **Yang** (1), Kevin R. **Chamberlain** (4), De-Fang **Wan** (5), Cun-Hua **Guo** (1), Xuan-Ce **Wang** (1) and Hua **Tao** (5)

(1) State Key Laboratory of Lithospheric Evolution, Institute of Geology and Geophysics, Chinese Academy of Sciences, Beijing 100027, China
(2) Key Laboratory of Isotope Geochronology and Geochemistry, Guangzhou Institute of Geochemistry, Chinese Academy of Sciences, Guangzhou 510640, China
(3) CAS Key Laboratory of Crust-Mantle Materials and Environments, School of Earth and Space Sciences, University of Science and Technology of China, Hefei 230026, China
(4) Department of Geology and Geophysics, University of Wyoming, Laramie, WY 82071, USA
(5) Institute of Mineral Resources, Chinese Academy of Geological Sciences, Beijing 100037, China
* Corresponding author. e-mail: lixh@gig.ac.cn

We introduce a potential new working reference material – natural zircon megacrysts from an Early Pliocene alkaline basalt (from Penglai, northern Hainan Island, southern China) – for the microbeam determination of O and Hf isotopes, and U–Pb age dating. The Penglai zircon megacrysts were found to be fairly homogeneous in Hf and O isotopes based on large numbers of measurements by LA-multiple collector (MC)-ICP-MS and SIMS, respectively. Precise determinations of O isotopes by isotope ratio mass spectrometry (IRMS) and Hf isotopes by solution MC-ICP-MS were in good agreement with the statistical mean of microbeam measurements. The mean $\delta^{18}O$ value of 5.31 ± 0.10‰ (2*s*) by IRMS and the mean $^{176}Hf/^{177}Hf$ value of 0.282906 ± 0.0000010 (2*s*) by solution MC-ICP-MS are the best reference values for the Penglai zircons. SIMS and isotope dilution-TIMS measurements yielded consistent $^{206}Pb/^{238}U$ ages within analytical uncertainties, and the preferred $^{206}Pb/^{238}U$ age was found to be 4.4 ± 0.1 Ma (95% confidence interval). The young age and variably high common Pb content make the Penglai zircons unsuitable as a primary U–Pb age reference material for calibration of unknown samples by microbeam analysis; however, they can be used as a secondary working reference material for quality control of U–Pb age determination for young (particularly ‹ 10 Ma) zircon samples.

Nous proposons un nouveau matériel de référence potentiel – des mégacristaux de zircon naturel provenant d'un basalte alcalin du début du pliocène (région de Penglai, nord de l'île de Hainan, Chine méridionale) destiné à l'analyse microfaisceaux des isotopes de l'O et de l'Hf, et la datation U–Pb. Les mégacristaux de zircon de Penglai se sont révélés, après un grand nombre de mesures par LA-MC-ICP-MS et SIMS, assez homogènes en terme d'isotopes de l'O et de l'Hf. Les déterminations précises des isotopes de l'O par IRMS et des isotopes de l'Hf par MC-ICP-MS solution sont en bon accord avec la moyenne statistique des analyses microfaisceaux. La valeur moyenne $\delta^{18}O$ de 5.31 ± 0.10‰ (2s) par IRMS et la valeur moyenne $^{176}Hf/^{177}Hf$ de 0.282906 ± 0.0000010 (2s) par solution MC-ICP-MS sont les meilleures valeurs de référence pour les zircons de Penglai. Les mesures SIMS ainsi que celles par dilution isotopique-TIMS donnent, compte tenu des incertitudes analytiques, des âges $^{206}Pb/^{238}U$ conformes, et l'âge préféré $^{206}Pb/^{238}U$ est estimé à 4.4 ± 0.10 Ma (intervalle de confiance de 95%). Leur jeune âge et leurs teneurs variables et élevées en Pb commun font que les zircons de Penglai ne sont pas utilisables comme matériel de référence primaire pour l'étalonnage d'échantillons inconnus dont les âges U–Pb doivent être déterminés par analyses microfaisceaux; Toutefois, ils peuvent être utilisés comme matériel de référence secondaire

GEOSTANDARDS and GEOANALYTICAL RESEARCH

Keywords: Zircon reference material, Penglai, U–Pb age, Hf isotopes, O isotopes, SIMS, LA-MC-ICP-MS.

Received 30 Jan 09 – Accepted 07 Sep 09

pour le contrôle qualité de la détermination de l'âge U–Pb des zircons jeunes (en particulier pour ceux ‹ 10 Ma).

Mots-clés : zircons de référence, Penglai, ages U–Pb, isotopes de l'Hf, isotopes de l'O, SIMS, LA-MC-ICP-MS.

Zircon is a common U-rich accessory mineral occurring in a wide range of rocks. Zircon is an excellent mineral for *in situ* U–Pb dating and O–Hf isotopic studies using modern techniques such as SIMS and LA-ICP-MS, but matrix effects are major limitations of these analytical methods. Therefore, the availability of well-characterised natural zircon reference materials is fundamental for accurate microbeam measurements. Ideal zircon reference materials would be homogeneous in both U–Pb age and O–Hf isotopic compositions, as well as being available in quantity to the scientific community. Although there are several well-characterised, natural zircon reference materials, such as SL13, 91500 and Temora, which have been used widely for microbeam analyses of U–Pb age and to lesser extent Hf–O isotopes (e.g., Wiedenbeck *et al.* 1995, 2004, Compston 1999, Horn *et al.* 2000, Black *et al.* 2004, Goolaerts *et al.* 2004, Blichert-Toft 2008, Ickert *et al.* 2008), these are limited in quantity or come from relatively inaccessible rock outcrops, to meet the demand of an increasing number of LA-ICP-MS facilities. We report here new U–Pb age and O–Hf isotopic results for the Penglai zircon megacrysts, hosted in Early Pliocene alkaline basalts from Hainan Island (China). Our data suggest that the Penglai zircons can be used as a new reference material for microbeam determination of O and Hf isotopes, as well as a quality control reference material for microbeam U–Pb age determinations of young (particularly ‹ 10 Ma) unknown samples.

Geological background and sample description

The Penglai zircons occur as megacrysts in the Early Pliocene alkaline basalts from northern Hainan Island of South China. These alkaline basalts were previously dated at 4.4–3.6 Ma by K–Ar and Ar–Ar techniques (Ge *et al.* 1989, Zhu and Wang 1989, Ho *et al.* 2000). As well as the zircon megacrysts, trace quantities of sapphire crystals occur sporadically in these alkaline basalts.

Qiu *et al.* (2005) carried out comprehensive *in situ* determinations of Lu–Hf isotopes (196 analyses on eight samples) and trace elements on the Penglai zircon megacrysts. They found that these mantle zircon megacrysts are characterised by relatively high U contents (mostly › 30 μg g^{-1}) and Th/U ratios (› 0.4), similar to the zircons found in the MARID-type xenoliths within kimberlites formed during mantle metasomatism (Konzett *et al.* 2000). Although the measured $^{176}Hf/^{177}Hf$ values varied from 0.282817 ± 0.000038 (1*s*) to 0.282991 ± 0.000034 (1*s*), 189 of 196 measurements fell within a relatively small range from 0.282851 ± 0.000030 to 0.282967 ± 0.000034 (1*s*). All the measured values formed a Gaussian distribution, with a grand mean of 0.282916 ± 0.000056 (2*s*), suggesting that the Penglai zircon megacrysts may be homogeneous in Hf isotopes.

The Penglai zircon megacrysts are highly abundant (visible to the naked eye) with nearly unlimited quantities on the weathered surfaces of basalts near the Penglai Town (19°30′55″N, 110°32′12″E), from where we collected *ca.* 800 g of zircon grains. These megacrysts are mostly several to over 10 mm long, translucent and maroon in colour (Figure 1a, b). Most Penglai zircon megacrysts are homogeneous, with only weak, broad zoning in cathodoluminescence (CL) images (Figure 1c–e). A few zircon shards displayed strong zoning in CL images; however, certain grains displayed dark domains (Figure 1f) that indicate high abundances of trace elements [U, Th and rare earth element (REE)].

Analytical methods

SIMS U–Pb zircon dating

Zircon shards, together with the 91500 and Temora-2 zircon reference materials, were placed in epoxy mounts which were then polished to section the crystals in half. All zircons were documented with transmitted and reflected light micrographs as well as CL images to reveal their

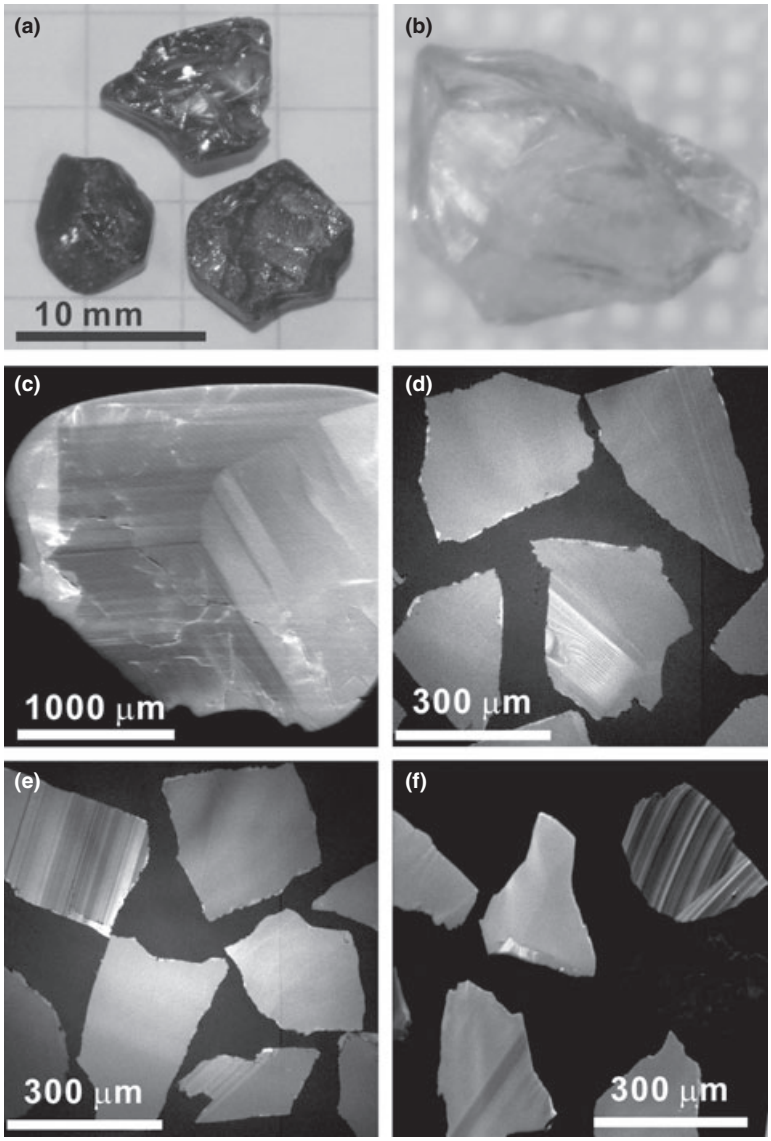

Figure 1. (a) Photographs of the Penglai zircon megacrysts. (b) Representative photomicrograph of Penglai zircon shards analysed by ID-TIMS (zA f4). The grid beneath the grains has 100 μm fibres with 150 μm openings; (c) representative CL image of Penglai zircon megacrysts; (d–f) representative CL images of Penglai zircon shards.

internal structures, and the mounts were vacuum-coated with high-purity gold.

Measurements of U, Th and Pb were conducted using the Chinese Academy of Sciences Cameca IMS-1280 ion microprobe (CASIMS) at the Institute of Geology and Geophysics (Beijing). The analytical procedures were similar to those described by Li *et al.* (2009). The O_2^- primary ion beam was accelerated at -13 kV, with an intensity of *ca.* 10 nA. The ellipsoidal spot was about 20 μm × 30 μm in size. Positive secondary ions were extracted with a 10 kV potential. Oxygen flooding was used to increase the O_2 pressure to *ca.* 5×10^{-6} Torr in the sample chamber, enhancing Pb^+ sensitivity to a value of ≥ 25 cps nA^{-1} per μg g^{-1}.

In the secondary ion beam optics, a 60 eV energy window was used, together with a mass resolution of *ca.* 5400 to separate Pb^+ peaks from isobaric interferences. The field aperture was set to 7000 μm, and the transfer optic magnification was adjusted to 200. Rectangular lenses were activated in the secondary ion optics to increase the transmission at high mass resolution. A single electron multiplier was used in ion-counting mode to measure secondary ion beam intensities by peak jumping. U–Th–Pb ratios were determined relative to the 1065 Ma 91500 zircon reference material with Th and U concentrations of *ca.* 29 and 81 μg g^{-1}, respectively (Wiedenbeck *et al.* 1995). Analyses of the 91500 zircon were interspersed with unknown grains. Because the Penglai zircons are very young (*ca.* 4.4 Ma) with very low radiogenic Pb, we list the measured (common Pb-uncorrected) isotopic ratios as well as the ^{207}Pb-corrected $^{238}U/^{206}Pb$ ages in Table 1. Uncertainties on individual analyses are reported at the 1*s* level; mean ages for pooled $^{206}Pb/^{238}U$ results are quoted at the 95% confidence interval.

ID-TIMS U–Pb dating

Two large (0.16 g each) Penglai zircon crystals were hand crushed, and only clear internal shards were selected for dissolution and analysis (e.g., Figure 1b). Three shards were annealed at 850 °C for 48 hr and dissolved in two steps following the chemical abrasion method of Mattinson (2005). The first dissolution step used HF and HNO_3 in a 180 °C oven for 12 hr. The liquid was discarded, and the remaining grains were rinsed and cleaned in HCl and HNO_3. A mixed ^{205}Pb–^{233}U–^{235}U tracer solution (ET535) was added to the micro-bombs for isotope dilution (ID) determination of Pb and U, and final dissolution used HF and HNO_3 at 240 °C. The three chemically abraded shards were dissolved alongside four shards that had not been annealed. Total dissolution required 17 d in the oven using a Parr digestion cell.

Lead and U were chemically purified on ion exchange columns using the HCl method modified from Krogh (1973). Due to the large sample sizes (2–4 mg zircon per shard), the ionic load exceeded the capacity of the 100 µl ion exchange columns, and visible cakes were present in the Pb elutions after evaporation. Therefore, the Pb elutions were run through the columns twice. One shard (zE f1) required three passes. The multiple passes through ion exchange columns increased the total procedural Pb blank. Based on stable, long-term average blanks for the laboratory (*ca.* 3.5 pg) and the measured blank from this round, total procedural Pb blank was estimated at 5 pg for two passes. The smallest sample was 45 pg Pb (zA f5 CA), but most were 100 pg or more, so that the blank contribution was adequately swamped by that of the sample. There was a significant amount of common Pb in these analyses (8–22 pg including the blank) even though the concentrations of initial Pb were quite low (0.002 µg g^{-1}). Fortunately, the Pb isotopic compositions of the Pb blank at the University of Wyoming laboratory (18.719 ± 0.97, 15.662 ± 0.57, 38.226 ± 1.42 for $^{206}Pb/^{204}Pb$, $^{207}Pb/^{204}Pb$ and $^{208}Pb/^{204}Pb$, respectively) and whole rock measurements

Table 1.
SIMS U–Pb isotopic data

Sample/ spot no.	U (µg g^{-1})	Th (µg g^{-1})	Th/U	$^{206}Pb/^{204}Pb$ measured	f_{206}%	$^{238}U/^{206}Pb$	± 1*s* (%)	$^{207}Pb/^{206}Pb$	± 1*s* (%)	207-corr age (Ma)	± 1*s*
Penglai@1	81	68	0.84	63	27.7	1222	4.8	0.155	10.57	4.54	0.26
Penglai@2	83	61	0.73	46	40.3	1272	6.3	0.100	19.31	4.72	0.33
Penglai@3	77	55	0.71	80	23.3	1329	6.4	0.174	18.79	4.06	0.34
Penglai@4	55	33	0.59	79	23.7	1419	7.2	0.192	16.40	3.69	0.34
Penglai@5	57	33	0.59	41	45.1	1575	7.5	0.181	17.43	3.38	0.32
Penglai@6	54	31	0.58	41	45.6	1498	7.3	0.200	21.48	3.45	0.36
Penglai@7	44	26	0.59	554	3.4	1135	9.7	0.143	19.60	4.97	0.53
Penglai@8	40	22	0.55	105	17.8	1277	9.6	0.302	16.04	3.39	0.50
Penglai@9	42	24	0.56	60	31.3	1324	11.2	0.196	18.45	3.93	0.51
Penglai@10	68	49	0.73	25	75.2	1591	6.9	0.114	21.74	3.68	0.29
Penglai@11	72	51	0.70	58	32.5	1488	7.1	0.112	18.38	3.95	0.31
Penglai@12	14	5	0.37	33	57.2	935	12.0	0.371	21.26	4.02	0.92
Penglai@13	14	5	0.38	35	53.8	1074	11.9	0.305	25.37	4.01	0.80
Penglai@14	1297	242	0.19	8977	0.2	1440	2.1	0.057	5.89	4.40	0.10
Penglai@15	821	324	0.39	1393	1.3	1486	2.5	0.055	7.21	4.27	0.11
Penglai@16	35	18	0.53	35	54.2	1320	8.7	0.251	18.61	3.59	0.46
Penglai@17	38	20	0.51	59	31.9	1259	8.1	0.173	19.95	4.28	0.43
Penglai@18	37	19	0.52	97	19.3	1294	8.8	0.217	19.28	3.89	0.46
Penglai@19	56	28	0.50	38	49.8	1070	7.1	0.217	16.02	4.72	0.46
Penglai@20	58	29	0.50	30	63.1	1170	7.5	0.191	24.62	4.51	0.49
Penglai@21	54	27	0.50	45	41.9	1089	9.2	0.227	16.46	4.58	0.54
Penglai@22	30	16	0.52	75	25.0	904	9.2	0.392	16.62	4.00	0.81
Penglai@23	1144	741	0.65	356	5.3	1436	3.7	0.068	7.71	4.40	0.17
Penglai@24	502	747	1.49	102	18.4	1398	3.3	0.084	9.54	4.43	0.16
Penglai@25	139	125	0.90	60	31.2	1304	5.6	0.189	12.89	4.07	0.30
Penglai@26	264	240	0.91	223	7.9	1438	3.2	0.089	9.39	4.24	0.15
Penglai@27	257	240	0.93	166	10.5	1421	4.3	0.099	16.93	4.23	0.21
Penglai@28	33	18	0.54	71	24.5	1089	7.3	0.276	19.99	4.18	0.56
Penglai@29	43	24	0.57	33	53.0	1334	7.1	0.267	14.25	3.47	0.38
Penglai@30	88	59	0.67	49	35.4	1289	6.4	0.149	15.10	4.34	0.32
Penglai@31	24	11	0.47	19	90.9	966	9.6	0.291	16.04	4.58	0.65

$^{238}U/^{206}Pb$ and $^{207}Pb/^{206}Pb$ values are not corrected for common lead. f_{206}% is the fraction of ^{206}Pb that is common Pb in percent.

of the sample host basalts (18.656 ± 0.121, 15.594 ± 0.082, 38.851 ± 0.226 averages of twenty samples; Tu *et al.* 1991) were very similar, so the choice of how the total common Pb was split between blank and sample had a negligible effect on the calculated radiogenic Pb isotopic values. Uranium only required one pass through columns and the blank was estimated as 0.2 pg based on long-term monitoring. Lead and U isotopic determinations were performed on a Micromass Sector 54 thermal ionisation mass spectrometer at the University of Wyoming using silica gel for Pb runs and graphite on a separate rhenium filament to run U as a metal. Lead was determined in either static multi-collector mode with ^{204}Pb in a Daly-photomultiplier amplifier and all other masses in Faraday collectors, or in single collector-Daly multiplier mode. In two cases, both modes were used for Pb (zE f2 and zE f3), which yielded indistinguishable results. Mass discrimination was determined to be 0.060 ± 0.06% amu^{-1} for Pb runs in static mode, and 0.185 ± 0.06% amu^{-1} for Pb in single Daly mode based on replicate analyses of NIST SRM 981. Uranium mass discrimination was determined within each run using the measured ^{233}U/^{235}U value. All measured values were well-determined, with the lowest signals well above baseline levels. The results are listed in Table 2. Concordia co-ordinates, intercepts and uncertainties were calculated using the PbMacDat and ISOPLOT programmes, based on Ludwig (1988, 1991, 2003).

SIMS oxygen isotope measurement

Zircon oxygen isotopes were measured using CASIMS, with analytical procedures that were similar to those reported by Li *et al.* (2010). The Cs^+ primary ion beam was accelerated at 10 kV, with an intensity of *ca.* 2 nA (Gaussian mode with a primary beam aperture of 200 μm to reduce aberrations) and rastered over a 10 μm area. The spot size was about 20 μm in diameter. The normal incidence electron flood gun was used to compensate for sample charging. Negative secondary ions were extracted with a -10 kV potential. Oxygen isotopes were measured using multi-collection mode. The mass resolution used to measure oxygen isotopes was *ca.* 2500. The nuclear magnetic resonance probe was used for magnetic field control with stability better than 3 ppm over 16 hr on mass 17. Measured ^{18}O/^{16}O ratios were normalised using Vienna Standard Mean Ocean Water compositions (VSMOW; ^{18}O/^{16}O = 0.0020052), and then corrected for the instrumental mass fractionation factor (IMF) as follows:

$$(\delta^{18}O)_M = \left(\frac{(^{18}O/^{16}O)_M}{0.0020052} - 1\right) \times 1000(‰), \quad (1)$$

$$IMF = (\delta^{18}O)_{M(reference)} - (\delta^{18}O)_{VSMOW}, \quad (2)$$

$$\delta^{18}O_{sample} = (\delta^{18}O)_M - IMF. \quad (3)$$

In this way, the results are reported in the conventional δ^{18}O notation with reference to VSMOW in per mil. With highly stable relative gain between two Faraday cup (FC) amplifiers, the reproducibility of the 91500 zircon reference samples was better than 0.26‰ (1*s*), and the internal precision of a single analysis was generally between 0.1‰ and 0.3‰ (2 SE), for ^{18}O/^{16}O ratios. The IMF was corrected using the 91500 zircon as a reference sample with a δ^{18}O value of 9.9‰ (Wiedenbeck *et al.* 2004).

SIMS oxygen isotopic determinations were carried out in three sessions. The first session was performed as individual measurements on ninety-one Penglai zircon shards on the same mount used for the SIMS U–Pb determination to examine inter-grain variability. After U–Pb dating, the sample mount was re-ground and re-polished to ensure that any oxygen implanted in the zircon surface from the O_2^- beam used for the U–Pb determination was removed. During the course of the first analytical session, the Temora-2 zircon reference material was also measured as an unknown together with the Penglai zircon. Ten measurements of Temora-2 yielded a weighted mean for δ^{18}O of 8.14 ± 0.20‰ (2*s*), which is consistent within error of the reported value of 8.20‰ (Black *et al.* 2004). A second session consisted of 113 individual measurements on 113 zircon shards. These two sessions were designed to identify any inter-grain variation in O isotopes. A third session was carried out undertaking profile analyses on nine megacrysts that crossed multiple CL domains to identify any intra-grain variations. All of the SIMS oxygen isotopic data are listed in Table S1, and a summary of these determinations are presented in Table 3.

Isotope ratio mass spectrometry (IRMS) oxygen isotope measurement

Laser fluorination technique: Oxygen was extracted from *ca.* 2 mg of the Penglai zircon megacrysts by the laser fluorination method (Sharp 1990, Rumble *et al.* 1997), and then directly analysed on a Finnigan Delta XP mass spectrometer at the CAS Key Laboratory of Crust-Mantle Materials and Environments, the University of Science and Technology of China, Hefei. A 25 W CO_2 laser (λ = 10.6 μm) and BrF_5 reagent were employed to extract O_2 for a direct measurement of ^{18}O/^{16}O ratios on the mass spectrometer (Zheng *et al.* 2002). Garnet UWG-2

Table 2.
TIMS U–Pb zircon data

Sample	Mass (mg)	U (μg g^{-1})	Sample Pb (μg g^{-1})	Sample Pb (pg)	Initial Pb (μg g^{-1})		Pb*/Pbc	f_{c206}%	Th/U	Corrected atomic ratios								^{206}Pb/^{238}U Age		^{207}Pb/^{235}U Age	
										^{206}Pb/^{204}Pb	^{208}Pb/^{206}Pb	^{206}Pb/^{238}U (rad.)	%err	^{207}Pb/^{235}U (rad.)	%err	^{207}Pb/^{206}Pb (rad.)	%err	Ma	err	Ma	err
3D total Pb linear intercept date = 4.36 ± 0.10 Ma (MSWD = 5.5); 206Pb/238U weighted mean date = 4.393 ± 0.041 95% confidence interval (MSWD = 188)																					
zA f1&2 CA *st*	3.05	40.8	0.034	103	0.004	10.8	5.9	3.6	0.69	520	0.22	0.0006760	(0.17)	0.004765	(1.22)	0.0511	(1.14)	4.357	± 0.007	4.826	8*P8/100
zA f3 *st*	2.73	48.2	0.042	114	0.006	16.5	4.5	5.2	0.70	362	0.23	0.0006728	(0.12)	0.004561	(1.10)	0.0492	(1.02)	4.336	± 0.005	4.620	± 0.051
zA f4 *st*	3.38	36.1	0.030	100	0.003	9.7	6.1	3.3	0.64	570	0.21	0.0006834	(0.15)	0.004742	(1.17)	0.0503	(1.09)	4.404	± 0.007	4.803	± 0.056
zA f5 CA *sD*	2.20	26.1	0.020	45	0.001	3.2	5.1	2.3	0.56	818	0.18	0.0006895	(0.21)	0.004674	(2.36)	0.0492	(2.18)	4.443	± 0.009	4.735	± 0.112
zE f1 CA *sD*	4.23	33.7	0.028	120	0.004	15.3	4.7	4.4	0.59	429	0.19	0.0006898	(0.14)	0.004705	(1.36)	0.0495	(1.26)	4.445	± 0.006	4.766	± 0.065
zE f2 *sD*	3.06	45.1	0.037	113	0.003	9.1	7.4	2.7	0.69	688	0.22	0.0006859	(0.11)	0.004759	(0.96)	0.0503	(0.89)	4.420	± 0.005	4.820	± 0.046
zE f3 *sD*	2.08	26.7	0.026	55	0.007	14.1	2.1	9.8	0.61	190	0.20	0.0006783	(0.22)	0.004565	(2.57)	0.0488	(2.39)	4.371	± 0.010	4.625	± 0.119
Paired static run data																					
zE f2 *st*	3.06	45.1	0.037	113	0.003	9.0	7.4	2.4	0.69	690	0.22	0.0006851	(0.11)	0.004741	(0.97)	0.0502	(0.90)	4.415	± 0.005	4.803	± 0.047
zE f3 *st*	2.08	26.7	0.026	54	0.007	13.9	2.1	9.8	0.61	192	0.20	0.0006781	(0.22)	0.004569	(2.57)	0.0489	(2.39)	4.370	± 0.010	4.629	± 0.119

Sample: z, zircon grain crushed; f, fragment (shard) analysed; CA, chemically abraded; *st*, static Pb run; *sD*, single Daly multiplier Pb run. Paired static data are from static Pb runs on the same beads after single Daly analysis. Mass: zircon fragment mass prior to first step of either CA-TIMS or total dissolution. U and Pb concentrations for CA method fragments are based on this mass and may be underestimates, depending on how much material was dissolved and leached in the first step. Picogram (pg) sample and initial Pb from the second dissolution step were measured directly. The masses and concentrations from the four bulk dissolved fragments are all accurate. Sample Pb: sample Pb (radiogenic + initial) corrected for laboratory blank of 5 pg, except for zE f1 CA which was run through columns three times and corrected for 7 pg. Initial Pb: common Pb corrected for laboratory blank of 5 pg Pb. Isotopic composition of blank = 18.719 ± 0.97 (^{206}Pb/^{204}Pb), 15.662 ± 0.57 (^{207}Pb/^{204}Pb) and 38.226 ± 1.42 (^{208}Pb/^{204}Pb). Pb*/Pbc: radiogenic Pb to total common Pb (blank + initial). f_{c206}%: fraction of blank-corrected, sample ^{206}Pb that is common in percent. Th/U calculated from radiogenic ^{208}Pb/^{206}Pb and ^{206}Pb/^{238}U date. meas.: measured ^{206}Pb/^{204}Pb corrected for mass discrimination and tracer. Corrected atomic ratios: ^{206}Pb/^{204}Pb corrected for blank, mass discrimination and tracer, all others corrected for blank, mass discrimination, tracer and initial Pb, values in parentheses are 2*s* uncertainties in percent. Isotopic composition of initial Pb = 18.656 ± 0.121, 15.594 ± 0.082, 38.851 ± 0.226, based on twenty whole rock measurements of Hainan basalts (Tu *et al.* 1991).

Table 3.
Summary of oxygen isotope data for Penglai zircons

	$\delta^{18}O$ (‰)	1*s*	Anal. numbers
SIMS			
Penglai-1@1-91 (individual analysis)	5.26	0.22	91
Penglai-2@1-113 (individual analysis)	5.31	0.17	113
Grain 5-1 (intra-grain profile analysis)	5.32	0.24	38
Grain 5-2 (intra-grain profile analysis)	5.25	0.27	15
Grain 5-3 (intra-grain profile analysis)	5.24	0.21	17
Grain 5-4 (intra-grain profile analysis)	5.21	0.23	10
Grain 5-5 (intra-grain profile analysis)	5.40	0.21	46
Grain 5-6 (intra-grain profile analysis)	5.41	0.20	18
Grain 5-7 (intra-grain profile analysis)	5.36	0.18	22
Grain 5-8 (intra-grain profile analysis)	5.21	0.26	36
Grain 5-9 (intra-grain profile analysis)	5.13	0.17	23
Laser fluorination	5.31	0.06	24
Traditioal BrF_5	5.31	0.07	3

with a $\delta^{18}O$ value of 5.8‰ (Valley *et al.* 1995) was used as the external reference material, and garnet 04BXL07 with a $\delta^{18}O$ value of 3.7‰ (Gong *et al.* 2007) was used as an in-house reference sample. Replicate analyses of these reference samples typically showed a daily standard deviation of about ± 0.1‰ (1*s*) for $\delta^{18}O$. Raw data were corrected to the 91500 zircon RM with a $\delta^{18}O$ value of 9.9‰ (Wiedenbeck *et al.* 2004).

Traditional BrF_5 technique: Oxygen isotope determinations were also performed in this study using the traditional BrF_5 technique (Clayton and Mayeda 1963) at the Institute of Mineral Resources, Chinese Academy of Geological Sciences in Beijing. Oxygen was liberated from *ca.* 10 mg of the Penglai zircon megacrysts by reaction with BrF_5 in nickel reaction vessels at 600 °C. The oxygen was purified and reduced to CO_2 using a vacuum extraction line similar to that described by Clayton and Mayeda (1963). The oxygen yield was determined by comparing the starting weight of mineral with the number of micromoles of gas produced. A Finnigan MAT-253 mass spectrometer was used to analyse the CO_2 with a working reference sample calibrated against the international reference material NBS 28 that gives $\delta^{18}O$ = 9.6‰. The external precision of the $\delta^{18}O$ measurement was ± 0.1‰ based on repeated analyses of reference samples. The IRMS zircon oxygen isotopic data are presented in Table S2.

MC-ICP-MS Hf isotope measurement

Hafnium isotopic determination was carried out on a Neptune, multi-collector, ICP-MS equipped with a Geolas-193 laser ablation system at the Institute of Geology and Geophysics (Beijing). The analytical conditions involved an ablation pit of 63 μm diameter, an ablation time of 26 s, a repetition rate of 10 Hz and a laser beam energy density of 10 J cm^{-2}. The detailed analytical procedures were similar to those described by Wu *et al.* (2006).

A total of 1286 measurements of Lu–Hf isotopes were carried out in five sessions by LA-MC-ICP-MS. In the first session, fifty-three measurements were made randomly on the eight zircon shards that had been previously analysed for U–Pb and O isotopes. An additional 343, 305 and 358 measurements were conducted randomly on thirty-four, thirty-two and thirty-four zircon megacrysts in the second, third and fourth sessions, respectively. In the fifth session, 226 measurements were made on nine zircon megacrysts that had been measured for oxygen isotopes as profile analyses, with laser spots being positioned near the spots used for SIMS determination of oxygen. Measured $^{176}Hf/^{177}Hf$ ratios were normalised to $^{179}Hf/^{177}Hf$ = 0.7325. No further external adjustments were applied to the unknowns because our determined $^{176}Hf/^{177}Hf$ ratios for the 91500 zircon (0.282302 ± 0.000020, 2*s*), as well as the Temora-2 zircon (0.282677 ± 0.000018, 2*s*) in session 1, were in good agreement with the reported values (e.g., Goolaerts *et al.* 2004, Wu *et al.* 2006, Blichert-Toft 2008).

Fifty-six Hf isotope measurements were also carried out by solution MC-ICP-MS by digestion of eleven crystals. The procedures for the separation of Hf from Zr and REE were similar to those reported by Goolaerts *et al.* (2004). The complete Lu–Hf isotopic data set is presented in Table S3, and a summary of these analyses is presented in Table 4.

Results

SIMS U–Pb age

Thirty-one analyses of thirty-one zircon shards were obtained during a single analytical session. Most analyses showed low Th concentrations that ranged from 5 to 68 μg g^{-1} and for U, from 14 to 88 μg g^{-1}, with a few exceptions that yielded high Th (125–747 μg g^{-1}) and U (139–1297 μg g^{-1}). Th/U ratios were mostly between 0.4 and 0.9, apart from spots 14 and 24, which gave values of 0.19 and 1.49, respectively.

Common Pb was variably high for the majority of analyses, with f_{206} values (the proportion of common ^{206}Pb in total measured ^{206}Pb) between 18.4% and 90.9%. Five of thirty-one analyses (spots 7, 14, 15, 23, 24 and 26) had relatively low common Pb, with f_{206}

Table 4.
Summary of Hf isotope data for Penglai zircons

Sample no.	$^{176}Yb/^{177}Hf$	1*s*	$^{176}Lu/^{177}Hf$	1*s*	$^{176}Hf/^{177}Hf$	1*s*	Anal. numbers
LA-MC-ICP-MS method							
Session 1							
Grain 1-1	0.0116	0.0003	0.000317	0.000010	0.282912	0.000007	20
Grain 1-2	0.0125	0.0008	0.000353	0.000028	0.282904	0.000009	5
Grain 1-3	0.0111	0.0002	0.000298	0.000002	0.282909	0.000014	5
Grain 1-4	0.0090	0.0009	0.000281	0.000029	0.282896	0.000007	5
Grain 1-5	0.0085	0.0040	0.000265	0.000118	0.282905	0.000007	5
Grain 1-6	0.0090	0.0038	0.000252	0.000106	0.282883	0.000006	4
Grain 1-7	0.0122	0.0002	0.000385	0.000007	0.282906	0.000014	4
Grain 1-8	0.0114	0.0001	0.000375	0.000003	0.282912	0.000013	5
Session 2							
Grain 2-1	0.0138	0.0015	0.000360	0.000038	0.282908	0.000010	10
Grain 2-2	0.0285	0.0078	0.000732	0.000187	0.282910	0.000013	10
Grain 2-3	0.0117	0.0034	0.000309	0.000086	0.282914	0.000015	9
Grain 2-4	0.0133	0.0018	0.000365	0.000047	0.282917	0.000016	9
Grain 2-5	0.0047	0.0006	0.000128	0.000015	0.282927	0.000013	10
Grain 2-6	0.0149	0.0051	0.000405	0.000140	0.282922	0.000009	10
Grain 2-7	0.0142	0.0064	0.000371	0.000166	0.282905	0.000015	10
Grain 2-8	0.0121	0.0027	0.000302	0.000064	0.282904	0.000012	10
Grain 2-9	0.0256	0.0165	0.000607	0.000361	0.282921	0.000012	13
Grain 2-10	0.0184	0.0115	0.000474	0.000269	0.282913	0.000017	12
Grain 2-11	0.0129	0.0080	0.000330	0.000194	0.282917	0.000019	10
Grain 2-12	0.0156	0.0033	0.000389	0.000078	0.282908	0.000017	10
Grain 2-13	0.0206	0.0097	0.000512	0.000229	0.282920	0.000013	9
Grain 2-14	0.0181	0.0044	0.000453	0.000102	0.282912	0.000012	11
Grain 2-15	0.0118	0.0062	0.000293	0.000150	0.282909	0.000013	11
Grain 2-16	0.0162	0.0086	0.000417	0.000224	0.282912	0.000011	9
Grain 2-17	0.0171	0.0052	0.000429	0.000130	0.282897	0.000013	10
Grain 2-18	0.0088	0.0034	0.000234	0.000080	0.282897	0.000020	9
Grain 2-19	0.0113	0.0010	0.000326	0.000024	0.282914	0.000016	10
Grain 2-20	0.0065	0.0034	0.000190	0.000098	0.282908	0.000013	10
Grain 2-21	0.0112	0.0014	0.000315	0.000037	0.282908	0.000017	10
Grain 2-22	0.0090	0.0032	0.000251	0.000088	0.282909	0.000008	10
Grain 2-23	0.0228	0.0058	0.000603	0.000147	0.282908	0.000012	10
Grain 2-24	0.0175	0.0068	0.000490	0.000178	0.282913	0.000013	11
Grain 2-25	0.0064	0.0014	0.000178	0.000038	0.282909	0.000013	10
Grain 2-26	0.0184	0.0050	0.000505	0.000133	0.282915	0.000013	10
Grain 2-27	0.0165	0.0073	0.000468	0.000204	0.282898	0.000013	10
Grain 2-28	0.0120	0.0052	0.000363	0.000155	0.282906	0.000010	10
Grain 2-29	0.0139	0.0060	0.000414	0.000171	0.282904	0.000012	10
Grain 2-30	0.0099	0.0024	0.000310	0.000074	0.282899	0.000013	10
Grain 2-31	0.0211	0.0030	0.000576	0.000076	0.282902	0.000020	10
Grain 2-32	0.0162	0.0072	0.000406	0.000163	0.282914	0.000018	10
Grain 2-33	0.0119	0.0053	0.000306	0.000132	0.282896	0.000012	10
Grain 2-34	0.0089	0.0017	0.000221	0.000041	0.282904	0.000014	10
Session 3							
Grain 3-1	0.0387	0.0022	0.000863	0.000043	0.282925	0.000009	9
Grain 3-2	0.0095	0.0011	0.000216	0.000025	0.282897	0.000011	11
Grain 3-3	0.0291	0.0105	0.000628	0.000208	0.282897	0.000014	10
Grain 3-4	0.0114	0.0030	0.000257	0.000065	0.282907	0.000021	10
Grain 3-5	0.0199	0.0041	0.000450	0.000090	0.282897	0.000014	10
Grain 3-6	0.0176	0.0038	0.000398	0.000086	0.282903	0.000020	10
Grain 3-7	0.0174	0.0091	0.000383	0.000195	0.282909	0.000021	10
Grain 3-8	0.0154	0.0036	0.000330	0.000063	0.282886	0.000014	10
Grain 3-9	0.0118	0.0015	0.000282	0.000036	0.282902	0.000019	10
Grain 3-10	0.0202	0.0187	0.000445	0.000372	0.282915	0.000020	9
Grain 3-11	0.0163	0.0007	0.000388	0.000016	0.282901	0.000016	10
Grain 3-12	0.0162	0.0014	0.000361	0.000031	0.282905	0.000014	9
Grain 3-13	0.0090	0.0020	0.000200	0.000040	0.282903	0.000015	10
Grain 3-14	0.0123	0.0039	0.000270	0.000085	0.282900	0.000017	9
Grain 3-15	0.0130	0.0091	0.000278	0.000192	0.282911	0.000018	10

Table 4 (continued).

Sample no.	$^{176}Yb/^{177}Hf$	1*s*	$^{176}Lu/^{177}Hf$	1*s*	$^{176}Hf/^{177}Hf$	1*s*	Anal. numbers
Grain 3-16	0.0224	0.0104	0.000467	0.000202	0.282910	0.000022	10
Grain 3-17	0.0117	0.0007	0.000255	0.000009	0.282881	0.000014	9
Grain 3-18	0.0135	0.0000	0.000293	0.000000	0.282883	0.000012	10
Grain 3-19	0.0081	0.0021	0.000229	0.000057	0.282895	0.000007	6
Grain 3-20	0.0092	0.0057	0.000271	0.000162	0.282917	0.000010	10
Grain 3-21	0.0108	0.0049	0.000342	0.000152	0.282914	0.000010	10
Grain 3-22	0.0145	0.0087	0.000448	0.000252	0.282913	0.000009	9
Grain 3-23	0.0155	0.0047	0.000458	0.000137	0.282910	0.000010	9
Grain 3-24	0.0136	0.0043	0.000418	0.000126	0.282917	0.000018	9
Grain 3-25	0.0132	0.0058	0.000392	0.000162	0.282904	0.000016	9
Grain 3-26	0.0123	0.0029	0.000371	0.000086	0.282910	0.000013	10
Grain 3-27	0.0136	0.0039	0.000387	0.000098	0.282907	0.000012	10
Grain 3-28	0.0125	0.0050	0.000364	0.000143	0.282902	0.000013	10
Grain 3-29	0.0093	0.0013	0.000271	0.000030	0.282909	0.000015	10
Grain 3-30	0.0117	0.0037	0.000340	0.000109	0.282912	0.000018	10
Grain 3-31	0.0103	0.0033	0.000313	0.000093	0.282918	0.000015	9
Grain 3-32	0.0066	0.0025	0.000216	0.000072	0.282897	0.000010	9
Session 4							
Grain 4-1	0.0243	0.0043	0.000619	0.000110	0.282915	0.000017	10
Grain 4-2	0.0202	0.0084	0.000506	0.000209	0.282915	0.000012	10
Grain 4-3	0.0144	0.0039	0.000380	0.000100	0.282901	0.000010	10
Grain 4-4	0.0229	0.0053	0.000603	0.000132	0.282897	0.000015	11
Grain 4-5	0.0111	0.0011	0.000298	0.000030	0.282902	0.000009	10
Grain 4-6	0.0119	0.0018	0.000308	0.000037	0.282904	0.000011	10
Grain 4-7	0.0286	0.0085	0.000755	0.000219	0.282911	0.000022	10
Grain 4-8	0.0155	0.0090	0.000418	0.000226	0.282896	0.000021	10
Grain 4-9	0.0082	0.0021	0.000222	0.000054	0.282889	0.000011	10
Grain 4-10	0.0215	0.0063	0.000585	0.000171	0.282884	0.000013	12
Grain 4-11	0.0156	0.0065	0.000406	0.000167	0.282914	0.000014	19
Grain 4-12	0.0072	0.0022	0.000187	0.000054	0.282900	0.000026	9
Grain 4-13	0.0149	0.0043	0.000403	0.000113	0.282914	0.000020	19
Grain 4-14	0.0113	0.0029	0.000315	0.000071	0.282912	0.000020	10
Grain 4-15	0.0092	0.0038	0.000260	0.000110	0.282899	0.000017	10
Grain 4-16	0.0110	0.0039	0.000301	0.000099	0.282902	0.000018	10
Grain 4-17	0.0141	0.0055	0.000391	0.000136	0.282907	0.000020	11
Grain 4-18	0.0129	0.0045	0.000368	0.000114	0.282910	0.000013	10
Grain 4-19	0.0267	0.0027	0.000739	0.000072	0.282902	0.000015	11
Grain 4-20	0.0052	0.0014	0.000149	0.000039	0.282908	0.000016	10
Grain 4-21	0.0194	0.0098	0.000557	0.000274	0.282911	0.000016	9
Grain 4-22	0.0240	0.0055	0.000630	0.000137	0.282906	0.000011	10
Grain 4-23	0.0124	0.0039	0.000361	0.000113	0.282913	0.000021	11
Grain 4-24	0.0125	0.0049	0.000366	0.000140	0.282904	0.000021	9
Grain 4-25	0.0056	0.0010	0.000157	0.000032	0.282901	0.000014	10
Grain 4-26	0.0238	0.0066	0.000710	0.000182	0.282918	0.000019	10
Grain 4-27	0.0094	0.0012	0.000289	0.000039	0.282907	0.000014	9
Grain 4-28	0.0071	0.0004	0.000218	0.000012	0.282912	0.000017	9
Grain 4-29	0.0121	0.0098	0.000371	0.000304	0.282909	0.000019	9
Grain 4-30	0.0111	0.0050	0.000335	0.000147	0.282905	0.000012	10
Grain 4-31	0.0064	0.0005	0.000191	0.000018	0.282909	0.000024	10
Grain 4-32	0.0128	0.0006	0.000346	0.000014	0.282904	0.000013	10
Grain 4-33	0.0110	0.0032	0.000327	0.000093	0.282904	0.000016	10
Grain 4-34	0.0318	0.0048	0.000897	0.000129	0.282901	0.000017	10
Session 5							
Grain 5-1	0.0089	0.0029	0.000286	0.000096	0.282914	0.000016	39
Grain 5-2	0.0093	0.0048	0.000300	0.000149	0.282905	0.000018	15
Grain 5-3	0.0106	0.0023	0.000336	0.000069	0.282897	0.000018	17
Grain 5-4	0.0082	0.0012	0.000270	0.000041	0.282907	0.000015	10
Grain 5-5	0.0075	0.0040	0.000233	0.000121	0.282899	0.000018	46
Grain 5-6	0.0199	0.0077	0.000601	0.000223	0.282910	0.000018	18
Grain 5-7	0.0108	0.0014	0.000359	0.000040	0.282901	0.000015	22
Grain 5-8	0.0169	0.0117	0.000529	0.000350	0.282909	0.000017	36
Grain 5-9	0.0125	0.0095	0.000392	0.000289	0.282917	0.000015	23

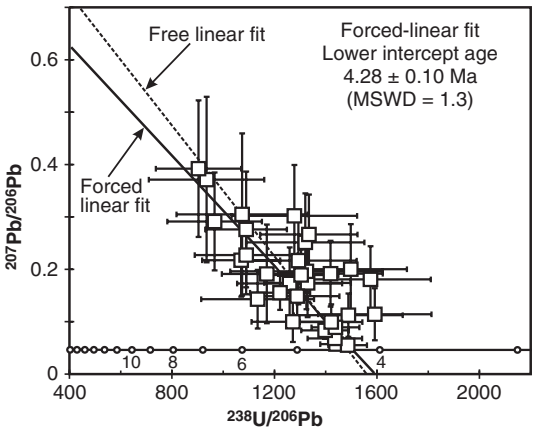

Figure 2. Tera–Wasserburg plot of SIMS analyses for Penglai zircon shards.

values ranging from 0.2% to 7.9%. Total Pb (not corrected for common Pb) $^{238}U/^{206}Pb$ and $^{207}Pb/^{206}Pb$ ratios were plotted on a Tera–Wasserburg plot (Figure 2) to avoid potential biases that could be introduced by calculating radiogenic Pb concordia co-ordinates from such common Pb-rich analyses. A free linear fit of all analyses on this plot yielded a lower-intercept age of 4.34 ± 0.13 Ma (95% confidence interval, mean square weighted deviation (MSWD) = 1.3) and an unreasonably old upper-intercept age of 5200 ± 330 Ma. Alternatively, a forced linear fit through an assumed common $^{207}Pb/^{206}Pb$ ratio of 0.8359 ± 0.0084 estimated from the zircon host basalt (Tu *et al.* 1991) yielded a lower-intercept age of 4.28 ± 0.10 Ma (95% confidence interval, MSWD = 1.3; Figure 2). Because of higher ^{207}Pb signal intensities compared with ^{204}Pb, the ^{207}Pb-correction method was used to calculate $^{238}U/^{206}Pb$ dates. The ^{207}Pb-corrected $^{238}U/^{206}Pb$ ages were relatively constant, ranging from 3.38 ± 0.32 to 4.97 ± 0.53 Ma (1*s*), with a weighted mean (one outlier) of 4.26 ± 0.10 Ma (95% confidence interval, MSWD = 1.2). It is noteworthy that spots 14, 15, 23 and 24 had high U concentrations between 502 and 1297 μg g^{-1}, and yielded the most precise $^{238}U/^{206}Pb$ ages of 4.40 ± 0.10, 4.27 ± 0.11, 4.40 ± 0.17 and 4.43 ± 0.16 Ma (1*s*). The weighted mean of these four analyses was 4.36 ± 0.12 Ma (95% confidence interval, MSWD = 0.34), which is in agreement within error with both lower-intercept ages (4.34 ± 0.13 and 4.28 ± 0.10 Ma).

To evaluate SIMS U–Pb data quality of the Penglai zircon calibrated against the 91500 zircon reference material, Temora-2 was alternately analysed as an unknown together with the Penglai zircon. Fifteen measurements of U–Pb isotopes were obtained for Temora-2. Analytical data are presented in Table S4. All the analyses were concordant within analytical uncertainties, yielding a concordia age (Ludwig 1998) of 417.0 ± 3.2 Ma (Figure S1), which is identical within error with the recommended value of 416.78 ± 0.33 Ma (Black *et al.* 2004). This result indicates that the calibration of Pb/U fractionation for the Penglai zircon material should be equally accurate, and the potential isobaric interference on mass 204 (such as ^{204}Hg and $^{176}Hf^{28}Si$) that will result in 'overestimation of ^{204}Pb' was negligible.

ID-TIMS U–Pb age

Uranium concentrations ranged from 27 to 48 μg g^{-1}, consistent with the majority of the SIMS analyses, sample Pb from 0.020 to 0.042 μg g^{-1}, and initial common Pb from 0.001 to 0.007 μg g^{-1} (2.3–9.8% of sample ^{206}Pb). The lower variation and lower absolute amounts of common Pb revealed in the TIMS data compared with the SIMS data set may reflect the fact that the TIMS analyses were derived from internal shards of only two zircon megacrysts. There were no significant differences in U, Pb or common Pb concentrations between the total bulk dissolutions and the second final step from those dissolved by the CA-TIMS method (Mattinson 2005). The similarity in spread of the concentrations of these two groups probably reflects the fact that there were very few metamict domains in these grains, based on the low U concentrations and young ages.

The data clustered near the concordia line with significant variations in $^{206}Pb/^{238}U$ and $^{207}Pb/^{235}U$ dates (Figure 3). The total range in $^{206}Pb/^{238}U$ dates was 0.11 Myr (or 2.5%). This variation may not be detectible by SIMS or LA-ICP-MS methods due to their lower analytical precisions. The spread in the $^{206}Pb/^{238}U$ dates may also reflect slight inheritance or problems with the ID measurements. These samples were somewhat under spiked, but there was no systematic relationship between the measured ID values and the resulting $^{206}Pb/^{238}U$ dates, so analytical difficulties seem unlikely. The lowest ion signal in each ID ratio was kept well above the baseline value in all cases (10–20 mV of ^{235}U and 30–100 mV ^{205}Pb typically).

The variation in $^{207}Pb/^{235}U$ dates and apparent discordance of the data could reflect slight inheritance, inaccurate measurements of the $^{206}Pb/^{204}Pb$ and/or $^{206}Pb/^{207}Pb$ ratios, inappropriate Pb blank amount or isotopic compositions, or an incorrect choice of initial $^{207}Pb/^{204}Pb$ compositions. Again, ^{207}Pb and ^{204}Pb intensities

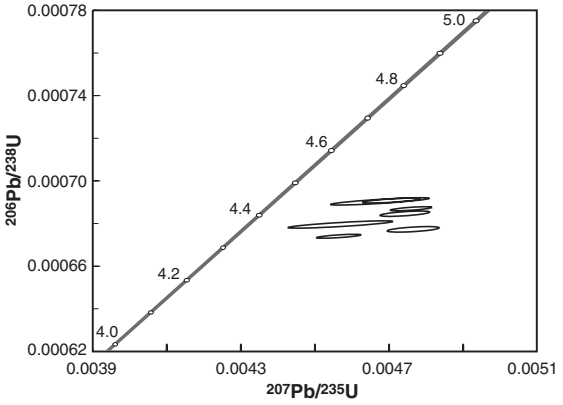

Figure 3. Conventional Wetherill concordia plot of TIMS analyses from individual, interior shards of two zircon crystals from the Penglai intrusion.

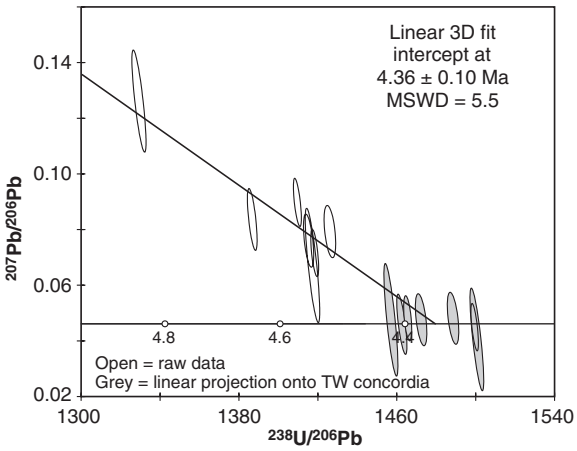

Figure 4. Tera–Wasserburg style 3D concordia plot for Penglai zircon shards of TIMS data using blank-corrected, total Pb values. The third axis is $^{204}Pb/^{206}Pb$. Calculated initial Pb isotopic compositions from this linear fit are 22 ± 11 for $^{206}Pb/^{204}Pb$ and 17.3 ± 6.5 for $^{207}Pb/^{204}Pb$.

were kept well above baseline values during all of these measurements: ^{207}Pb was typically 40–20 mV for static Faraday runs, 100000 cps or more for single Daly runs, ^{204}Pb was 3000 cps or more in both modes, and any potential interferences from organic molecules were monitored and removed before acquiring data. The magnitudes of the analytical inaccuracies necessary to explain the discordance were 6% for $^{206}Pb/^{207}Pb$ measurements and 10% for $^{206}Pb/^{204}Pb$. Biases of these magnitudes do not seem realistic. For two of the analyses, zE f2 and zE f3, data were acquired in both single Daly and static multi-collector mode and the reduced data from the paired sets were indistinguishable. The Pb blank at the University of Wyoming laboratory was well-determined and stable. Both the Pb isotopic composition and total procedural blank amounts were measured with each dissolution batch. The isotopic composition of the Pb blank at the University of Wyoming was very similar to the whole rock Pb isotopic values of Hainan basalts from the sample area (Tu *et al.* 1991), so there was a negligible effect on the calculated concordia co-ordinates based on how the measured common Pb was split between blank and initial Pb.

To evaluate whether the choice of initial Pb isotopic compositions was controlling the apparent discordance, blank-corrected total Pb values were plotted in a 3D scheme (Ludwig 2003) with $^{204}Pb/^{206}Pb$ as the *z*-axis on a Tera–Wasserburg plot (Figure 4). A linear fit on this plot yielded an intercept date of 4.36 ± 0.10 Ma (95% confidence interval, MSWD = 5.5), and initial $^{206}Pb/^{204}Pb$ = 22 ± 11 and $^{207}/Pb/^{204}Pb$ = 17.3 ± 6.5. The intercept date from a 2D Tera–Wasserburg plot of radiogenic Pb (corrected using Hainan basalt values for common Pb isotopic compositions) was 4.41 ± 0.22 Ma (95% confidence interval, MSWD = 7.7), within error of the total Pb 3D intercept date. The similarity of these dates demonstrates that the choice of initial Pb isotopic compositions did not skew the calculated intercept date significantly.

The best estimates of the zircon U–Pb age come from the 3D intercept date of 4.36 ± 0.10 Ma (95% confidence interval, MSWD = 5.5) and the weighted mean $^{206}Pb/^{238}U$ date of 4.393 ± 0.041 (95% confidence interval, MSWD = 188), both of which were consistent with the SIMS U–Pb age of 4.28 ± 0.10 Ma (lower-intercept age of all analyses) and 4.36 ± 0.12 (average of four high U determinations) within analytical error. The tentatively preferred age is 4.4 ± 0.1 Ma (95% confidence interval).

SIMS oxygen isotope data

Ninety-one individual SIMS measurements of oxygen isotopes were conducted on ninety-one zircon shards (including thirty-one zircon shards that were dated by SIMS U–Pb measurements) in the first session. Values of $\delta^{18}O$ ranged from 4.74‰ to 5.73‰, forming a Gaussian distribution with a grand mean of 5.26 ± 0.44‰ (2*s*; Figure 5a). The second session comprised 113 individual measurements of 113 zircon shards. The measured $\delta^{18}O$ values were between 4.86‰ and 5.74‰, forming a Gaussian distribution with a grand mean of 5.31 ± 0.35‰ (2*s*; Figure 5b).

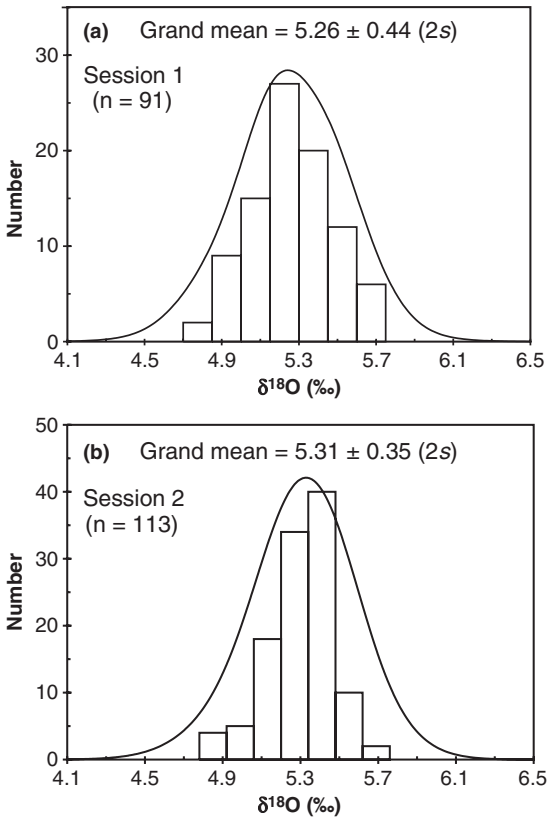

Figure 5. Histogram of $\delta^{18}O$ values for Penglai zircon shards determined by SIMS in session 1 (a) and session 2 (b) relative to the 91500 zircon reference material with a $\delta^{18}O$ value of 9.9 (Wiedenbeck *et al.* 2004).

Profile analyses, comprising 225 oxygen isotope measurements, were conducted on nine zircon megacrysts in the second session. Figure 6a and d shows the CL images of two representative Penglai megacrysts (Grain 5-1 and Grain 5-9) for profile analyses, and the measured $\delta^{18}O$ values are plotted against each transect in Figure 6b and e. The measured $\delta^{18}O$ values in Grains 5-1 and 5-9 showed no correlation with different CL domains, yielding grand means of 5.32 ± 0.47‰ and 5.13 ± 0.34‰, respectively. Overall, all the 225 measured $\delta^{18}O$ values for the nine megacrysts were between 4.75‰ and 5.86‰, forming a Gaussian distribution with a grand mean of 5.30 ± 0.46‰ (2*s*; Figure 7a) comparable with the results of the individual measurements for 204 shards in the first and second sessions. The averages of intra-grain profiles from each of the nine grains varied from 5.13 ± 0.17‰ (1*s*) to 5.41 ± 0.20‰ (1*s*; Table 3), yielding a mean of 5.28 ± 0.19‰ (2*s*; Figure 7b). These results suggest a rather small intra-grain variation of oxygen isotopes within individual megacrysts.

Overall, both the inter-grain individual and intra-grain profile measurements were corroborative and indicate that Penglai megacrysts are fairly homogeneous in oxygen isotopes. The grand mean of $\delta^{18}O$ value for all 316 SIMS measurements was 5.29 ± 0.46‰ (2*s*), which is consistent with the value of 5.3 ± 0.6‰ (2*s*) for normal mantle zircons (e.g., Valley *et al.* 1998, Page *et al.* 2007).

IRMS oxygen isotope data

Twenty-four measurements of oxygen isotopes were conducted on twelve zircon shards by the laser fluorination technique. Values of $\delta^{18}O$ ranged from 5.24‰ to 5.38‰ (Table 3), forming a Gaussian distribution with a grand mean of 5.31 ± 0.12‰ (2*s*; Figure 8). Three measurements by the conventional BrF_5 technique yielded a mean value of 5.31 ± 0.14‰ (2*s*; Table 3) that is identical with the results obtained by laser fluorination and SIMS within analytical uncertainties. All IRMS analyses gave a mean value of $\delta^{18}O$ of 5.31 ± 0.10‰ (2*s*), which is interpreted as the best reference value for the Penglai zircons.

LA-MC-ICP-MS Hf isotope data

LA-MC-ICP-MS analyses comprising a total of 1286 Lu–Hf isotope measurements were undertaken in five sessions. Because the measured $^{176}Yb/^{177}Hf$ ratio values were relatively high (› 0.001), independent mass bias factors for Hf and Yb in the isobaric interference correction were used to produce more reliable Hf isotopic data (Woodhead *et al.* 2004, Iizuka and Hirata 2005, Wu *et al.* 2006). Fifty-three Lu-Hf isotopic measurements were made on eight zircon shards in session 1. The measured $^{176}Hf/^{177}Hf$ values ranged from 0.282878 ± 0.000014 (1*s*) to 0.282932 ± 0.000014 (1*s*), forming a Gaussian distribution with a grand mean of 0.282906 ± 0.000024 (2*s*; Figure 9a).

Sessions 2, 3 and 4 comprised 343, 305 and 358 random Lu-Hf isotopic measurements on 34, 32 and 34 zircon megacrysts, respectively. Overall, the 1006 measured $^{176}Hf/^{177}Hf$ values ranged from 0.282864 ± 0.000022 (1*s*) to 0.282949 ± 0.000019 (1*s*; Table S3). The measured $^{176}Hf/^{177}Hf$ values for both intra-grain and inter-grain analyses of each sessions formed Gaussian distributions, with grand means of 0.282910 ± 0.000030 (2*s*), 0.282905 ± 0.000034 (2*s*) and 0.282906 ± 0.000036 (2*s*) for sessions 2, 3 and 4, respectively (Figure 9b–d).

Session 5 yielded 225 Lu-Hf isotopic measurements from nine zircon megacrysts along the profiles of previous

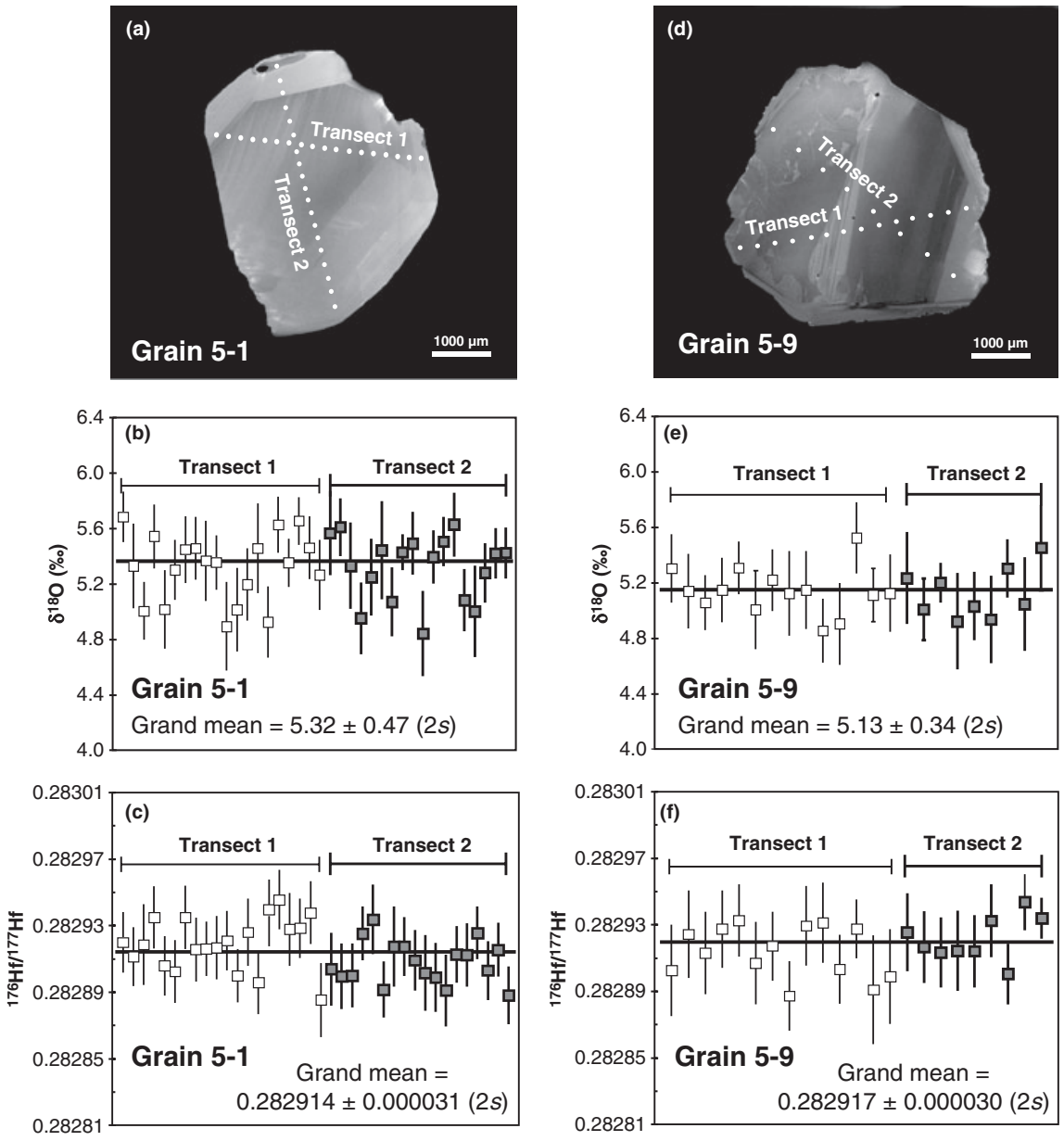

Figure 6. Cathodoluminescence images and profile analyses of O–Hf isotope measurements transecting different CL domains for two representative Penglai zircon megacrysts (Grain 5-1 and Grain 5-9). Small white dots within the CL images indicate the analytical spots of Hf isotopes by LA-MC-ICP-MS. Corresponding analytical spots of SIMS oxygen isotope measurements, which are too small to be shown, are near the spots of Hf isotopes. The measured $\delta^{18}O$ values were calibrated relative to the 91500 zircon reference material with a $\delta^{18}O$ value of 9.9 (Wiedenbeck *et al.* 2004).

measurements for oxygen isotopes. The measured $^{176}Hf/^{177}Hf$ values for two representative Penglai megacrysts, Grains 5-1 and 5-9, are plotted against each transect in Figure 6c and f. No correlations were observed between the measured $^{176}Hf/^{177}Hf$ values in Grains 5-1 and 5-9 relative to different CL domains, and the two grains yielded grand means of 0.282914 ± 0.000031 (2*s*) and 0.282917 ± 0.000030 (2*s*), respectively. All 225 measured $^{176}Hf/^{177}Hf$ values from the nine megacrysts ranged from 0.282861 ± 0.000017 (1*s*) to 0.282953 ± 0.000013 (1*s*), and formed a Gaussian distribution with a grand mean of 0.282907 ± 0.000036 (2*s*; Figure 9e).

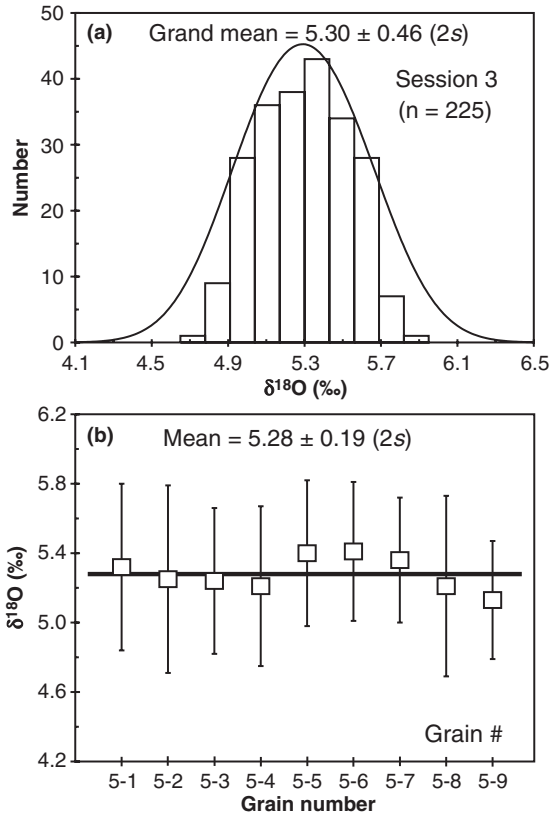

Figure 7. (a) Histogram of intra-grain $\delta^{18}O$ measurements for the Penglai zircon megacrysts in session 3. (b) Average of intra-grain $\delta^{18}O$ values for each megacryst in session 3. Error bars are 2*s*. The measured $\delta^{18}O$ values were calibrated relative to the 91500 zircon reference material with an $\delta^{18}O$ value of 9.9 (Wiedenbeck *et al.* 2004).

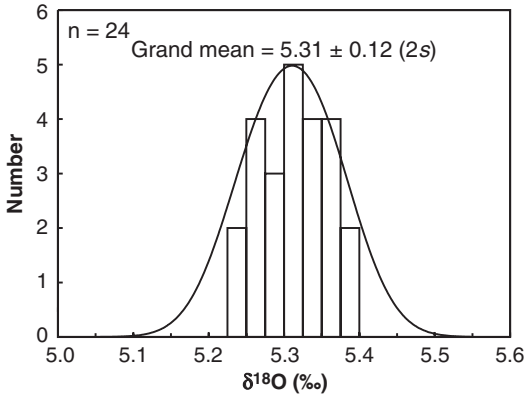

Figure 8. Histogram of $\delta^{18}O$ values for the Penglai zircon shards determined by the laser fluorination IRMS technique relative to the 91500 zircon reference material with a $\delta^{18}O$ value of 9.9 (Wiedenbeck *et al.* 2004).

Results of all 1286 measurements on 117 zircon megacrysts/shards also formed a Gaussian distribution with a grand mean of 0.282907 ± 0.000034 (2*s*; Figure 9f). Averages of 117 intra-grain $^{176}Hf/^{177}Hf$ measurements in sessions 1–5 varied from 0.282881 ± 0.000014 (1*s*) to 0.282927 ± 0.000013 (1*s*; (Table 4), with a mean of 0.282906 ± 0.000016 (2*s*; Figure 10). This result, with improved precision, is indistinguishable within uncertainty from the average value of 0.282916 ± 0.000056 (2*s*) reported by Qiu *et al.* (2005). Therefore, the Penglai zircon megacrysts are fairly homogeneous in Hf isotopes and appear to lack any significant intra- and inter-grain variations.

Solution MC-ICP-MS Hf isotope data

Eleven zircon megacrysts were dissolved for chemical purification of Hf, and fifty-six solution MC-ICP-MS measurements were conducted on the purified Hf dissolution. The measured $^{176}Hf/^{177}Hf$ values were between 0.282892 ± 0.000012 and 0.282919 ± 0.000009 (2 SE). All $^{176}Hf/^{177}Hf$ data formed a Gaussian distribution with a grand mean of 0.282906 ± 0.000024 (2*s*; Figure 11a). The mean of $^{176}Hf/^{177}Hf$ values determined by solution MC-ICP-MS for eleven megacrysts was 0.282906 ± 0.000010 (2*s*; Figure 11b), which is identical with the statistical mean of the laser ablation results.

We tentatively conclude that the Penglai zircon megacrysts have reasonably homogeneous Hf isotopic compositions, based on both the laser ablation and solution measurements conducted in this study, as well as the previous data of Qiu *et al.* (2005). The mean value of $^{176}Hf/^{177}Hf$ = 0.282906 ± 0.000010 (2*s*) of solution MC-ICP-MS measurements is the preferred reference value for the Penglai zircons.

Conclusions

This study has demonstrated that the Penglai zircon megacrysts are fairly homogeneous in Hf and O isotopic composition. Variations in Hf and O isotopic compositions as determined by LA-MC-ICP-MS and SIMS, respectively, did not exceed experimental uncertainties. Precise measurements by solution MC-ICP-MS for Hf isotopes and by IRMS for O isotopes were very consistent with the statistical means of microbeam (LA-MC-ICP-MS and SIMS) measurements. Thereby, the Penglai zircon megacrysts can be used as a suitable working reference material for Hf and O isotopes for the microbeam analysis of unknown zircon samples. A major advantage of the Penglai zircon megacrysts

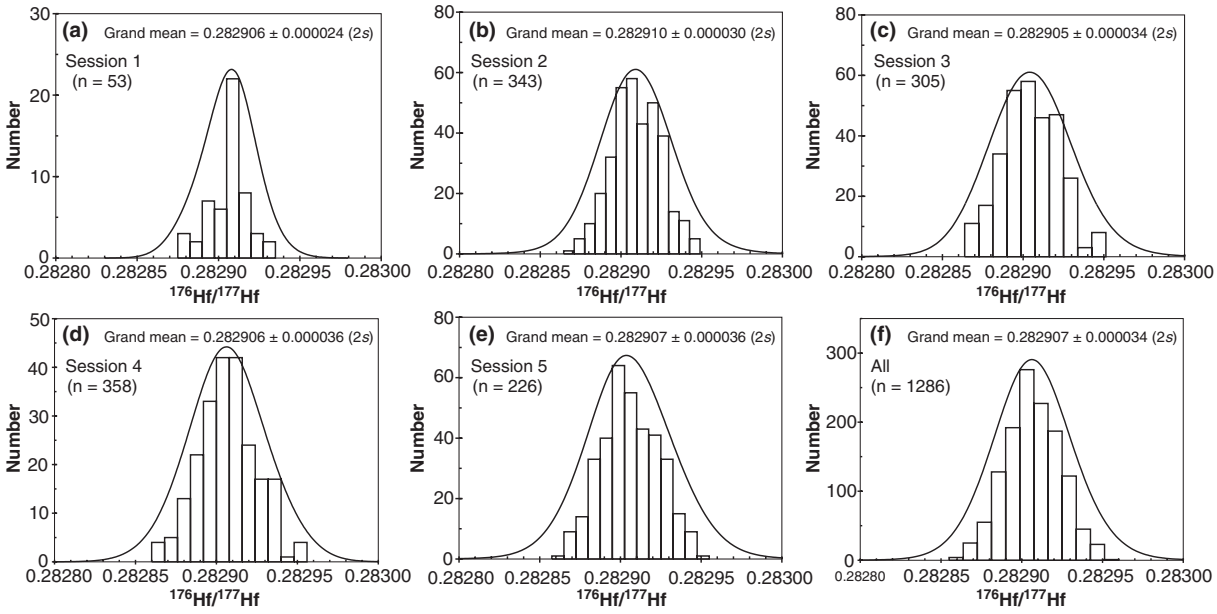

Figure 9. Histogram of $^{176}Hf/^{177}Hf$ ratios determined by LA-MC-ICP-MS for Penglai zircon shards and/or megacrysts in each analytical session 1–5 (a–e) and all five sessions (f).

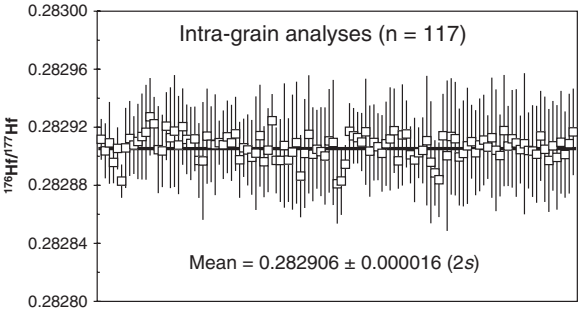

Figure 10. Average of intra-grain $^{176}Hf/^{177}Hf$ measurements for 117 zircon grains in sessions 1–5 determined by LA-MC-ICP-MS. Each datum point is the mean of the measured $^{176}Hf/^{177}Hf$ values within each zircon grain. Error bars are 2*s*.

is the easy access to the field locality and the almost unlimited quantity of zircon that can be made available to the international geoscience community.

Reference zircons with U–Pb ages younger than 5 Ma are rare (see summary of Sláma *et al.* 2008). The Penglai zircons appear to be homogeneous in U–Pb age. The age uncertainty is relatively large (2.5%) because the zircons contain variably high levels of non-radiogenic Pb, and low U and Pb concentrations relative to other zircon reference

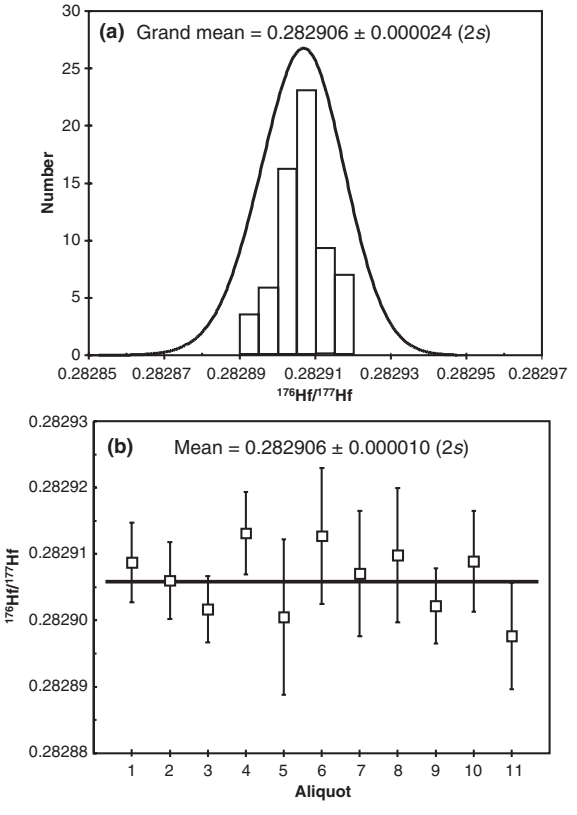

Figure 11. Average of intra-grain $^{176}Hf/^{177}Hf$ measurements determined by solution MC-ICP-MS. Error bars are 2*s*.

materials of Palaeozoic and Precambrian ages. These characteristics lead to low count rates and poor counting statistics for microbeam analyses. Alternatively, there could be a real, small variation in zircon age on the order of 0.1 Ma, in view of the ID-TIMS measurements, which awaits further investigation.

Although the Penglai zircons may be too young and contain variably high amounts of common Pb to be a suitable U–Pb age reference material for calibration of unknown samples by microbeam analysis, the material can be used as a secondary working reference material for quality control of U–Pb age determination of young (particularly ‹ 10 Ma) zircon samples.

There are currently 800 g of Penglai zircon megacrysts available for distribution. These are stored in the SIMS laboratory at the Institute of Geology and Geophysics, Chinese Academy of Science in Beijing, and are available on request from the lead author of this article.

Acknowledgements

We appreciate the assistance of Y.Y. Gao and W. Dan for assistance with SIMS oxygen and LA-MC-ICP-MS hafnium isotopic determinations, and two anonymous referees for constructive reviews of the article. This work is jointly supported by the Ministry of Science and Technology of China (grants 2007AA06Z126 and 2007CB411403) and the Institute of Geology and Geophysics, Chinese Academy of Sciences (grant Z0908).

References

Black L.P., Kamo S.L., Allen C.M., Davis D.W., Aleinikoff J.N., Valley J.W., Mundil R., Campbell I.H., Korsch R.J., Williams I.S. and Foudoulis C. (2004)
Improved $^{206}Pb/^{238}U$ microprobe geochronology by the monitoring of a trace-element-related matrix effect; SHRIMP, ID-TIMS, ELA-ICP-MS and oxygen isotope documentation for a series of zircon standards. **Chemical Geology, 205**, 115–140.

Blichert-Toft J. (2008)
The Hf isotopic composition of zircon reference material 91500. **Chemical Geology, 253**, 252–257.

Clayton R.N. and Mayeda T.K. (1963)
The use of bromine pentafluoride in the extraction of oxygen from oxides and silicates for isotopic analysis. **Geochimica et Cosmochimica Acta, 27**, 43–52.

Compston W. (1999)
Geological age by instrumental analysis: the 29th Hallimond Lecture. **Mineralogical Magazine, 63**, 297–311.

Ge T.M., Chen W.J., Xu X., Lee D.M., Fan L.M., Lee Q., Wen S.Y. and Wang X. (1989)
The geomagnetic polarity time scale of Quaternary for Leiqiong area. K-Ar dating and palaeomagnetic evidence from volcanic rocks. **Acta Geophysica Sinica, 32**, 550–557.

Gong B., Zheng Y.-F. and Chen R.-X. (2007)
TC/EA-MS online determination of hydrogen isotope composition and water concentration in eclogitic garnet. **Physics and Chemistry of Minerals, 34**, 687–698.

Goolaerts A., Mattielli N., Jong J.D., Weis D, James D. and Scoates J.S. (2004)
Hf and Lu isotopic reference values for the zircon standard 91500 by MC-ICP-MS. **Chemical Geology, 206**, 1–9.

Ho K.S., Chen J.C. and Juang W.S. (2000)
Geochronology and geochemistry of late Cenozoic basalts from the Leiqiong area, southern China. **Journal of Asian Earth Sciences, 18**, 307–324.

Horn I., Rudnick R.L. and McDonough W.F. (2000)
Precise elemental and isotope ratio determination by simultaneous solution nebulization and laser ablation-ICP-MS: application to U-Pb geochronology. **Chemical Geology, 164**, 2821–301.

Ickert R.B., Hiess J., Williams I.S., Holden P., Ireland T.R., Lanc P., Schram N., Foster J.J. and Clement S.W. (2008)
Determining high precision, *in situ*, oxygen isotope ratios with a SHRIMP II: analyses of MPI-DING silicate-glass reference materials and zircon from contrasting granites. **Chemical Geology, 257**, 114–128.

Iizuka T. and Hirata T. (2005)
Improvements of precision and accuracy in *in-situ* Hf isotope microanalysis of zircon using the laser ablation-MC-ICP-MS technique. **Chemical Geology, 220**, 121–137.

Konzett J., Armstrong R.A. and Günther D. (2000)
Modal metasomatism in the Kaapvaal craton lithosphere: constraints on timing and genesis from U-Pb zircon dating of metasomatised peridotites and MARID-type xenoliths. **Contributions to Mineralogy and Petrology, 139**, 704–719.

Krogh T.E. (1973)
A low-contamination method for hydrothermal decomposition of zircon and extraction of U and Pb for isotopic age determinations. **Geochimica et Cosmochimica Acta, 37**, 485–494.

Li X.H., Liu Y., Li Q.L., Guo C.H. and Chamberlain K.R. (2009)
Precise determination of Phanerozoic zircon Pb/Pb age by multi-collector SIMS without external standardization. **Geochemistry Geophysics Geosystems, 10**, Q04010, doi: 10.1029/2009GC002400.

Li X.H., Li W.X., Li Q.L., Wang X.C., Liu Y. and Yang Y.H. (2010)
Petrogenesis and tectonic significance of the ~850 Ma Gangbian alkaline complex in South China: evidence from *in situ* zircon U-Pb and Hf-O isotopes and whole-rock geochemistry. **Lithos, 114**, 1–15.

references

Ludwig K.R. (1988)
PBDAT for MS-DOS, a computer program for IBM-PC compatibles for processing raw Pb-U-Th isotope data, version 1.24. **U.S. Geological Survey, Open-File Report 88–542.**

Ludwig K.R. (1991)
ISOPLOT for MS-DOS, a plotting and regression program for radiogenic-isotope data, for IBM-PC compatible computers, version 2.75. **U.S. Geological Survey, Open-File Report 91–445,** 45pp.

Ludwig K.R. (1998)
On the treatment of concordant uranium-lead ages. **Geochimica et Cosmochimica Acta, 62**, 665–676.

Ludwig K.R. (2003)
ISOPLOT/Ex version 3.0, a geochronological toolkit for Microsoft Excel. **Geochronology Center Special Publication (Berkeley, CA, USA)**, vol. 4, 37pp.

Mattinson J.M (2005)
Zircon U-Pb chemical abrasion ("CA-TIMS") method: combined annealing and multi-step partial dissolution analysis for improved precision and accuracy of zircon ages. **Chemical Geology, 220**, 47–66.

Page F.Z., Fu B., Kita N.T., Fournelle J., Spicuzza M.J., Schulze D.J., Viljoen F., Basei M.A.S. and Valley J.W. (2007)
Zircons from kimberlite: new insights from oxygen isotopes, trace elements, and Ti in zircon thermometry. **Geochimica et Cosmochimica Acta, 71**, 3887–3903.

Qiu Z.L., Wu F.Y., Yu Q.Y., Xie L.W. and Yang S.F. (2005)
Hf isotopic compositions of zircon megacrysts in Cenozoic basalts from eastern China. **Chinese Science Bulletin, 50**, 2602–2611.

Rumble D., Farquhar J., Young E.D. and Christensen C.P. (1997)
In situ oxygen isotope analysis with an excimer laser using F_2 and BrF_5 reagents and O_2 gas as analyte. **Geochimica et Cosmochimica Acta, 61**, 4229–4234.

Sharp Z.D. (1990)
A laser-based microanalytical method for the *in situ* determination of oxygen isotope ratios of silicates and oxides. **Geochimica et Cosmochimica Acta, 54**, 1353–1357.

Sláma J., Kosler J., Condon D.J., Crowley J.L., Gerdes A., Hanchar J.M., Horstwood M.S.A., Morris G.A., Nasdala L., Norberg N., Schaltegger U., Schoene B., Tubrett M.N. and Whitehouse M.J. (2008)
Plesovice zircon – a new natural reference material for U-Pb and Hf isotopic microanalysis. **Chemical Geology, 249**, 1–35.

Tu K., Flower M.F., Carlson R.W., Zhang M. and Xie G. (1991)
Sr, Nd, and Pb isotopic compositions of Hainan basalts (south China): implications for a subcontinental lithosphere Dupal source. **Geology, 19**, 567–569.

Valley J.W., Kitchen N., Kohn M.J., Niendorf C.R. and Spicuzza M.J. (1995)
UWG-2, a garnet standard for oxygen isotope ratio: Strategies for high precision and accuracy with laser heating. **Geochimica et Cosmochimica Acta, 59**, 5223–5231.

Valley J.W., Kinny P.D., Schulze D.J. and Spicuzza M.J. (1998)
Zircon megacrysts from kimberlite: oxygen isotope variability among mantle melts. **Contributions to Mineralogy and Petrology, 133**, 1–11.

Wiedenbeck M., Allé P., Corfu F., Griffin W.L., Meier M., Oberli F., von Quadt A., Roddick J.C. and Speigel W. (1995)
Three natural zircon standards for U–Th–Pb, Lu–Hf, trace-element and REE analyses. **Geostandards Newsletter, 19**, 1–23.

Wiedenbeck M., Hanchar J.M., Peck W.H., Sylvester P., Valley J., Whitehouse M., Kronz A., Morishita Y., Nasdala L., Fiebig J., Franchi I., Girard J.P., Greenwood R.C., Hinton R., Kita N., Mason P.R.D., Norman M., Ogasawara M., Piccoli R., Rhede D., Satoh H., Schulz-Dobrick B., Skar O., Spicuzza M.J., Terada K., Tindle A., Togashi S., Vennemann T., Xie Q. and Zheng Y.F. (2004)
Further characterisation of the 91500 zircon crystal. **Geostandards and Geoanalytical Research, 28**, 9–39.

Woodhead J., Hergt J., Shelley M., Eggins S. and Kemp R. (2004)
Zircon Hf-isotope analysis with an excimer laser, depth profiling, ablation of complex geometries, and concomitant age estimation. **Chemical Geology, 209**, 121–135.

Wu F.Y., Yang Y.H., Xie L.W., Yang J.H. and Xu P. (2006)
Hf isotopic compositions of the standard zircons and baddeleyites used in U-Pb geochronology. **Chemical Geology, 234**, 105–126.

Zheng Y.F., Wang Z.R., Li S.G. and Zhao Z.F. (2002)
Oxygen isotope equilibrium between eclogite minerals and its constraints on mineral Sm-Nd chronometer. **Geochimica et Cosmochimica Acta, 66**, 625–634.

Zhu B.Q. and Wang H.F. (1989)
Nd-Sr-Pb isotopic and chemical evidence for the volcanism with MORB-OIB source characteristics in the Leiqiong area, China. **Geochimica (Beijing), 3**, 193–201.

Supporting information

The following supporting information is available as part of the online article (doi: 10.1111/j.1751-908X.2010.00036.x):

Figure S1. Concordia plot of SIMS U–Pb data for the Temora-2 zircon reference material.

Table S1. SIMS oxygen isotope data for the Penglai zircon

Table S2. IRMS oxygen isotope data for the Penglai zircon

Table S3. MC-ICP-MS Lu–Hf isotopic data

Table S4. SIMS U–Pb data for the Temora-2 zircon reference material

Please note: Blackwell Publishing are not responsible for the content or functionality of any supporting information supplied by the authors. Any queries (other than missing material) should be directed to the corresponding author for the article.